

PREPARATION AND STEADY-STATE HEAT TRANSFER CHARACTERISTICS ANALYSIS OF BUILDING INSULATION PHASE CHANGE COMPOSITE MATERIAL

by

Chengcai LIU^{a,b*}

^a School of Civil Engineering, Zhengzhou University of Technology,
Zhengzhou, Henan, China

^b Civil Engineering Evaluation Technology Research Center,
Zhengzhou, Henan, China

Original scientific paper
<https://doi.org/10.2298/TSCI2402329L>

The compatibility of $Ba(OH)_2 \cdot 8H_2O$ with aluminum alloy and copper after 50 heating cycles was studied using SEM and high power X-ray diffraction technique. Analyze the effect of temperature on thermal stability. The results show that $Ba(OH)_2 \cdot 8H_2O$ has some corrosion resistance to aluminum alloys and is similar with copper. The $Ba(OH)_2 \cdot 8H_2O$ /foam copper phase transition composites were prepared by a simple vacuum adsorption filling method. The experimental process of phase change energy storage device with and without copper foam was established, and the continuous heat transfer and transformation of $Ba(OH)_2 \cdot 8H_2O$ /foam copper phase change composites were carried out at room temperature. The results show that compared with pure $Ba(OH)_2 \cdot 8H_2O$, $Ba(OH)_2 \cdot 8H_2O$ /foam copper phase converter has faster heat transfer and better thermal conductivity, effectively reducing the supercooling effect of $Ba(OH)_2 \cdot 8H_2O$. Heat transfer experiment at high temperature shows that the heat capacity of $Ba(OH)_2 \cdot 8H_2O$ /foam copper phase changes with the increase of temperature. When the temperature of the zone is higher than the material phase changes in temperature, some insulation measures should be taken for phase shifting components.

Key words: $Ba(OH)_2 \cdot 8H_2O$, foam copper, phase transition, composite materials, heat transfer performance

Introduction

Currently, the development of the economy is closely related to the living standards of the people. In 2017, our Chinese government adjusted the economic growth rate to 6.5%, which sparked heated discussions in the global media [1]. However, economic development cannot do without energy consumption, especially fossil fuels. The consumption of fossil fuels not only generates a large amount of GHG emissions, causing global warming, but also leads to a series of climate and environmental issues. In June 2016, back propagation released a statistical yearbook of World energy resources after conducting a survey and statistics on World energy resources. The yearbook reveals that global energy consumption increased by 1% in 2015. Oil is still the fuel with the largest global demand (accounting for 32.9%), followed by coal (accounting for 29.2%), and natural gas accounts for 23.8% of primary energy consumption. Compared to other countries around the world, China has been the top country

* Author's e-mail: 20150235646@mail.sdufe.edu.cn

in the energy consumption growth market for 15 consecutive years. In China, energy consumption is currently dominated by Secondary sector of the economy and Tertiary sector of the economy, that is, the total energy consumption of industry and service industry in China has increased year by year from 2011 to 2015, reaching 430000 tons of standard coal in 2015, converting this number into electrical energy is very large. Among all energy consumption, the leading one is coal. The total annual consumption of coal is almost always over 2700000 tons of standard coal, and China's current proven coal stock is approximately 1.5 trillionns (2015 results) [2, 3]. Imagine if we consume at this rate every year, and within a few hundred years, we will consume all our coal resources. In addition, China is also a major user of automobiles. According to statistics, as of the end of 2016, the national car ownership had reached 194 million vehicles, which means a large amount of oil needs to be refined into gasoline. From 2011-2015, the total consumption of oil continued to grow, maintaining an annual consumption of 700 millionns of standard coal, a large part of which still relies on imports. By consulting information, burning one ton of standard coal will generate approximately 2.6 tons of carbon CO₂. If calculated according to this ratio, China emitted a total of approximately 11.18 billionns of CO₂ in 2015, and its impact is far-reaching and difficult to assess. With the intensification of energy scarcity, the storage, development, and utilization of renewable energy have become a focus of attention for countries. The energy storage cannot only reduce the total energy dissipation and unnecessary waste, but also improve the performance and reliability of the whole system. Among various energy storage methods, to take advantage of liquid-solid phase transfer materials such as constant-temperature phase and high latent pressure during the process of converter so as to achieve energy storage and comprehensive utilization in the field of solar energy, waste energy industry applications, *etc.*, to improve the quality of energy storage and utilization. Home energy conservation, and thermal energy resources analysis, become the research hotspot in the field of energy efficiency research and material science. Liquid phase change products mainly divided into two types: organic and inorganic. Paraffin is the most common organic PCM. Organic PCM are often not prone to undercooling and phase separation. The material has stable thermochemistry properties, low corrosivity, low toxicity and low cost. However, organic phase transfer materials have low thermal conductivity and are closely related to combustion in high temperature. Most inorganic phase transition materials are crystalline hydrated salt, which is a medium and low temperature phase transition energy storage material. When the temperature rises, the crystalline hydrated salt will be separated from water of crystallization make the salt dissolve and absorb heat [4]. When the temperature decreases, the reverse process occurs, absorbing water of crystallization and releasing heat. In order to eliminate or slow down its undercooling and suppress phase separation, the usual method is to add a certain amount of nucleating and thickening agents. This method requires testing and searching from a large number of materials, which requires a lot of time and effort. Therefore, restraining the undercooling of crystalline hydrates and improving their heat transfer performance have always been the focus of phase change energy storage technology research. Phase change integrated circuit device can overcome the shortage of phase change equipment and achieve the best application of phase change equipment. Therefore, the development of phase change energy storage technology has become a research hotspot in the area of phase change information science. Currently, MSC based on MSC are the most concerned systems. The metal base materials are Cu base (Cu foam), Al base (Al foam), Ni base (Ni foam), *etc.*, with low cost, excellent thermal conductivity and other characteristics. Phase change energy storage materials are a new type of PCM with high storage capacity, good stability and low price. This project intends to disperse

and integrate transformational substances into a foam network. The method takes advantage of the high latent heat of PCM and the high heat conduction characteristics of porous metal matrix, and uses the induced heat of metal matrix for heat storage. In addition, the metal skeleton divides the phase change energy storage material into numerous tiny heat storage units, overcoming the shortcomings of poor heat transfer performance of liquid mixtures during the transient process of solid phase transformation, and difficult to control the heat/discharge at certain temperature during the heating/discharge process [5, 6].

Methods

Experimental materials

The $\text{Ba}(\text{OH})_2 \cdot 8\text{H}_2\text{O}$ used in the experiment is produced by Sinopharm Chemical Reagent Co., Ltd., a Shanghai trial brand, and analytically pure. The filling material is foam copper with pore density (Pores Per Inch, PPI) of 10PPI and 25PPI, and porosity of 97.1% and 96.7%, respectively. The material is red Cu [7].

The $\text{Ba}(\text{OH})_2 \cdot 8\text{H}_2\text{O}$ /preparation of foam copper phase change composites

In addition ground $\text{Ba}(\text{OH})_2 \cdot 8\text{H}_2\text{O}$ phase change the intermediate material for the heat storage tank in the vacuum argon filling box, vacuum the argon filling box to the high purity vacuum system (no less than 1×10^{-2} Torr) by vacuum pump, and fill it with high purity argon. After the argon pressure is equal to the air, close the main argon filling valve. Conduct constant temperature water bath heating to realize direct and direct heating of phase change products. Provide foam copper bone cleanser after making into insulation box, so that foam copper can absorb phase change in molten state. The adsorption time is about 1 hour, and the adsorption rate accounts for 85–90% of the total theoretical collection rate of solid phase change. Wash the full length of foam copper adsorbed $\text{Ba}(\text{OH})_2 \cdot 8\text{H}_2\text{O}$ in cold state and integrate into the cleaning unit of phase change energy storage. The phase-change energy storage device equipped with foam copper is heated uniformly under the condition of vacuum argon filling, and the liquid $\text{Ba}(\text{OH})_2 \cdot 8\text{H}_2\text{O}$ is collected twice. Liquid phase $\text{Ba}(\text{OH})_2 \cdot 8\text{H}_2\text{O}$ was collected. Repeat this function and increase the collection of $\text{Ba}(\text{OH})_2 \cdot 8\text{H}_2\text{O}$ phase converter as much as possible [8].

Compatibility Experiment of $\text{Ba}(\text{OH})_2 \cdot 8\text{H}_2\text{O}$ with metal materials

Two metal test tubes with identical structural dimensions were designed and processed, made of red Cu and Al alloy. The $\text{Ba}(\text{OH})_2 \cdot 8\text{H}_2\text{O}$ PCM of the same quality was added to these two metal test tubes to make the metal container filled with phase change material work under long-term melting solidification phase change process and withstand significant thermal stress. The PCM will have a certain corrosion effect on the metal container material at high temperatures. During the compatibility experiment, Cu and Al alloy metal test tubes filled with $\text{Ba}(\text{OH})_2 \cdot 8\text{H}_2\text{O}$ were placed in a constant temperature water bath for thermal cycling experiments. Melting and solidification thermal cycling experiments were conducted between 50–95 °C. After 50 thermal cycling experiments, metal cross-sections at the same position were cut from different metal test tubes for SEM morphology analysis and EDS surface element analysis. Figure 1 is a schematic diagram of the compatibility experiment between $\text{Ba}(\text{OH})_2 \cdot 8\text{H}_2\text{O}$ and metal materials .

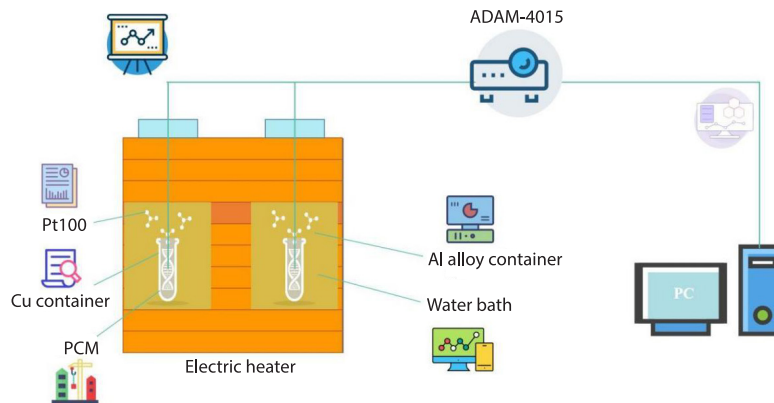


Figure 1. Schematic diagram of the compatibility experiment between $\text{Ba}(\text{OH})_2 \cdot 8\text{H}_2\text{O}$ and metal materials

The $\text{Ba}(\text{OH})_2 \cdot 8\text{H}_2\text{O}$ /heat transfer experiment of foam copper

The heat transfer experiment of $\text{Ba}(\text{OH})_2 \cdot 8\text{H}_2\text{O}$ solid phase change equipment includes the change of state and the change of unit temperature, as well as the steady-state experiment in the constant temperature unit. In this project, $\text{Ba}(\text{OH})_2 \cdot 8\text{H}_2\text{O}$ is used as the matrix to collect it by vacuum electron beam welding technology. The temperature stability test of the three-phase change energy storage device was carried out to compare its heat transfer characteristics. In this project, a new thin film electric heat pipe with an area equivalent to the phase-change energy storage base is proposed, and the controllable output of the electric heat pipe is realized by using the adjustable DC voltage regulator power supply. Six Pt100 modified thermistors were installed on the Pt100, and the temperature measurement error was within ± 0.1 °C. The temperature was measured at 2 seconds intervals.

Results and discussion

Compatibility of $\text{Ba}(\text{OH})_2 \cdot 8\text{H}_2\text{O}$ with metal materials

Figures 2 and 3 show the EDS spectra of the compatibility experiment between $\text{Ba}(\text{OH})_2 \cdot 8\text{H}_2\text{O}$ and Al alloy. From the EDS spectra of monitoring Point B located far away from $\text{Ba}(\text{OH})_2 \cdot 8\text{H}_2\text{O}$ and monitoring Point A located at the interface between $\text{Ba}(\text{OH})_2 \cdot 8\text{H}_2\text{O}$ and Al alloy, it can be seen that the content of Al element decreases while the content of O element increases, indicating the presence of Al_2O_3 at the interface between $\text{Ba}(\text{OH})_2 \cdot 8\text{H}_2\text{O}$ and Al alloy. At the same time, the content of Ba element reaches 9.54 wt.%, indicating a high enrichment content. Figures 4 and 5 show the EDS spectra of the compatibility experiment between $\text{Ba}(\text{OH})_2 \cdot 8\text{H}_2\text{O}$ and Cu. The main component of monitoring Point A is O 13.41 wt.%, Cu 86.59 wt.%, the main component of monitoring Point B is O 2.26 wt.%, Cu 97.74 wt.%, from the EDS spectra of monitoring Point B located far from $\text{Ba}(\text{OH})_2 \cdot 8\text{H}_2\text{O}$ and monitoring Point A located at the junction of $\text{Ba}(\text{OH})_2 \cdot 8\text{H}_2\text{O}$ and Cu, it can be seen that the content of element O slightly increases, while the decrease in Cu content is not significant, and there is no occurrence of Ba element.

In summary, Al alloys have high activity in strong alkaline solutions and can provide higher output current density and output power. Some alloy elements in Al alloys accelerate the local corrosion failure rate of defect locations with higher corrosion activity on the surface

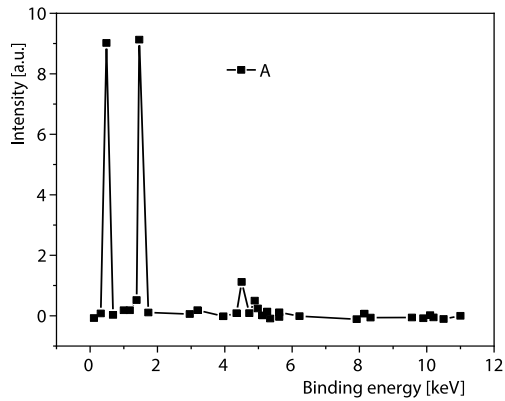


Figure 2. The EDS Spectrogram A of the compatibility experiment between $\text{Ba}(\text{OH})_2 \cdot 8\text{H}_2\text{O}$ and Al alloy

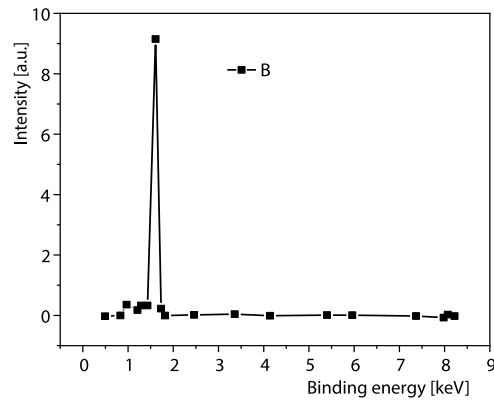


Figure 3. The EDS Spectrogram B of the compatibility experiment between $\text{Ba}(\text{OH})_2 \cdot 8\text{H}_2\text{O}$ and Al alloy

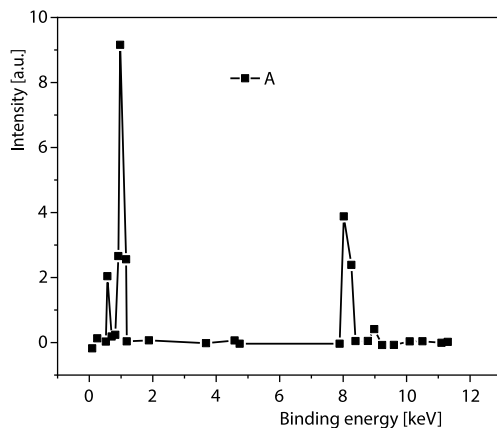


Figure 4. The EDS Spectrogram A of the compatibility experiment between $\text{Ba}(\text{OH})_2 \cdot 8\text{H}_2\text{O}$ and red Cu

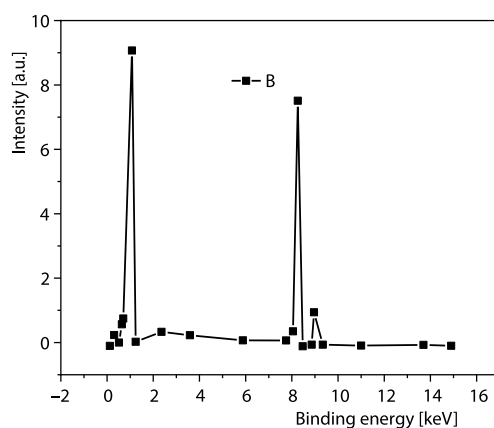


Figure 5. The EDS Spectrogram B of the compatibility experiment between $\text{Ba}(\text{OH})_2 \cdot 8\text{H}_2\text{O}$ and red Cu

due to corrosion tendency, making Al alloys more susceptible to strong corrosion in strong alkaline solutions. Red copper is prone to chemical reactions in strong alkaline solutions to generate more stable copper containing oxygen-containing compounds. With the formation of a passivation film on the surface of red copper, the corrosion active sites on the surface of red copper are reduced, preventing further corrosion of red copper and reducing the corrosion reaction rate. Therefore, Al alloy is prone to chemical reaction and corrosion with strong alkali $\text{Ba}(\text{OH})_2 \cdot 8\text{H}_2\text{O}$, Cu has strong corrosion resistance to $\text{Ba}(\text{OH})_2 \cdot 8\text{H}_2\text{O}$, which is consistent with the discussion on the relationship of $\text{Ba}(\text{OH})_2 \cdot 8\text{H}_2\text{O}$ with metal materials. Therefore, Cu alloy is used as filler for $\text{Ba}(\text{OH})_2 \cdot 8\text{H}_2\text{O}$ and metallic material for containers.

Steady-state experimental results of thermal storage and release of phase change energy storage devices with and without foam copper

The temperature and latent heat of $\text{Ba}(\text{OH})_2 \cdot 8\text{H}_2\text{O}$ phase shifter were measured using DSC method. Within the range of 26-105 °C, the temperature rises by 3 °C and the tempera-

ture rises by 3 °C. The high temperature-plated crucible can prevent the rapid crystallization of water by heating $\text{Ba}(\text{OH})_2 \cdot 8\text{H}_2\text{O}$ through purification from high purity nitrogen, reducing the thermal loss of the sample, and more accurately drawing the DSC curve of the sample. Figure 6 shows the DSC test curve of $\text{Ba}(\text{OH})_2 \cdot 8\text{H}_2\text{O}$ at liquid phase transition temperature of 78 °C. The latent heat of barium hydroxide $\text{Ba}(\text{OH})_2 \cdot 8\text{H}_2\text{O}$ aqueous solution was 284 J/g, calculated by endothermic peak area in DSC curve. In this project, $\text{Ba}(\text{OH})_2 \cdot 8\text{H}_2\text{O}$ without Cu foam and $\text{Ba}(\text{OH})_2 \cdot 8\text{H}_2\text{O}$ containing Cu foam were selected as the research object to study the heat release rule of $\text{Ba}(\text{OH})_2 \cdot 8\text{H}_2\text{O}$ at 80 W power and natural cooling at room temperature. Figure 7 shows an average wall temperature distribution on the upper surface of the sample. In the process of heat storage and temperature rise, the average top surface temperature of 10 PPI and 25 PPI phase change energy storage devices reached 86 °C at 4122 seconds and 3866 seconds, and the average top surface temperature without Cu foam reached 86 °C at 4764 seconds. The heat absorption process of 10 PPI was shortened by 642 seconds compared to 25 PPI Cu foam and 898 seconds compared to 25 PPI Cu foam. In this system, because of the high thermal conductivity of Cu foam, the heat transfer rate and heat storage time in the heat absorption process are greatly improved. The results show that the phase transition temperature of $\text{Ba}(\text{OH})_2 \cdot 8\text{H}_2\text{O}$ is about 78 °C, and the phase change energy storage device with or without Cu foam has a significant solid-liquid biphasic platform. The $\text{Ba}(\text{OH})_2 \cdot 8\text{H}_2\text{O}$ water is heated in solid-liquid form. In the solid-liquid two-phase region, the temperature of the 10 PPI Cu foam phase transition storage energy storage device increases from 78 °C (1480 seconds) to 82 °C (3680 seconds), and the temperature required by the 10 PPI Cu foam phase transition storage energy storage device is 2200 seconds. In the solid-liquid two-phase region 25, the temperature of PPI Cu foam phase change energy storage device rose from 78-82 °C in 1468 seconds, and 2126 seconds in 3594 seconds. In the liquid two-phase region, the temperature of the energy storage device without Cu foam was increased from 78 °C in 1998 to 82 °C now in 2220 seconds. During this phase change, the average temperature of the system rises rapidly, and the loss rate of the foam-containing Cu phase change energy storage material is similar to that of the non-foam-containing Cu phase change energy storage material. In the process of phase transformation, latent heat is the main factor. In liquid-solid two-phase region, the phase change heat storage devices with foam and without foam have the same characteristics of phase change heat storage. The results show that the speed adjustment of phase change energy storage material with Cu foam substrate is faster than that without Cu foam substrate during heating process. When the average temperature on the surface of the heat storage system drops from 86-50 °C, the phase change energy storage device without Cu foam needs 7189 seconds, and the 10 PPI and 25 PPI Cu foam composite phase change energy storage devices need 5816 seconds and 6464 seconds, respectively, which is 19.1% and 10.1%, Cu foam not only increased the thermal conductivity of PCM, but also greatly accelerated the solidification rate of PCM. The average wall temperature of the phase change energy storage device without Cu foam dropped to 68.8 °C, and the $\text{Ba}(\text{OH})_2 \cdot 8\text{H}_2\text{O}$ PCM began to crystallize rapidly, releasing latent heat. The undercooling degree was 8.2 °C, and the undercooling degrees of the 10 PPI and 25 PPI Cu foam composite phase change energy storage devices were reduced to 4 °C and 1 °C, respectively, indicating that the skeleton structure of Cu foam provided a nucleation site for the crystallization of hydrated salt, which could effectively reduce the undercooling degree of $\text{Ba}(\text{OH})_2 \cdot 8\text{H}_2\text{O}$ PCM, the Cu foam with larger pore density can provide more nucleation sites for crystalline hydrated salt and improve its nucleation ability [9, 10].

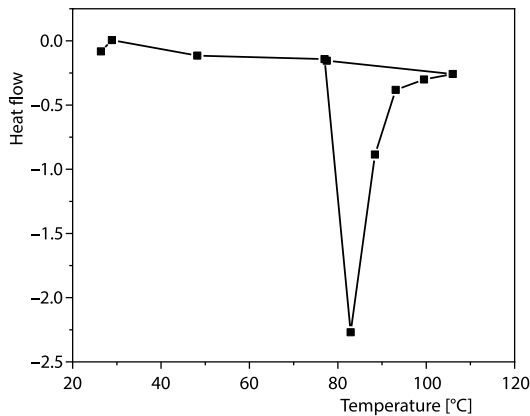


Figure 6. Differential scanning calorimetry (DSC) test curve of $\text{Ba}(\text{OH})_2 \cdot 8\text{H}_2\text{O}$

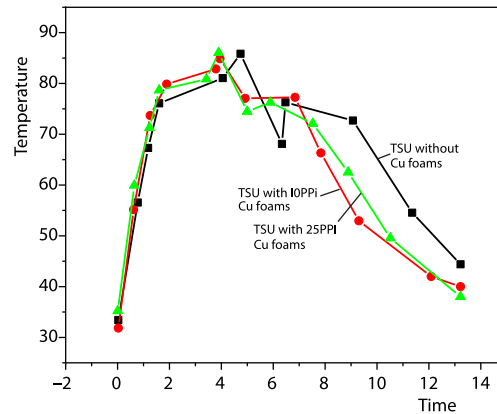


Figure 7. Average wall temperature curve of upper surface of phase change TSU test piece with and without Cu foam

Conclusion

The combination of $\text{Ba}(\text{OH})_2 \cdot 8\text{H}_2\text{O}$ with Cu and Al alloy steel shows that $\text{Ba}(\text{OH})_2 \cdot 8\text{H}_2\text{O}$ has some corrosion resistance on Al alloy, as well as copper. It's very good for copper. The phase change properties of foam metal composite adopts vacuum argon tank, which has good sealing effect, prevents the combination of pollutants with explosive materials such as air and water vapor, and is helpful for improving product quality. The high mixing ratio of Cu foam and vacuum secondary melt injection process ensures the full rate and distribution of different phase change products. The purpose of this project is to control the phase change information of $\text{Ba}(\text{OH})_2 \cdot 8\text{H}_2\text{O}$ /Cu foam by adjusting the characteristics of $\text{Ba}(\text{OH})_2 \cdot 8\text{H}_2\text{O}$ /Cu foam phase change method, and speed up the phase change information of $\text{Ba}(\text{OH})_2 \cdot 8\text{H}_2\text{O}$ /Cu foam phase change method. Moreover, the production efficiency is simple, the composition is high, and the efficiency is high. The $\text{Ba}(\text{OH})_2 \cdot 8\text{H}_2\text{O}$ /Cu foam phase converter has the advantages of high latent heat, fast heat preservation and low supercooling coefficient, which can solve the problems of supercooling and low thermal conductivity in long-term use of crystalline cement-based PCM. Under the same heat transfer condition, Cu foam with larger pore size is selected as filler, and its nucleation effect is better. The when using phase transformer storage device for constant power supply and temperature control, full consideration should be given to the heat absorbing/discharging time and the heat of phase converter.

Acknowledgment

The study was supported by A key R and D and extension project (Science and Technology research project) in Henan Province, 2023, Project No. 232102321073 – The experimental study on the performance of the Yellow River silt static compression ecological block.

References

- [1] Li, Y., *Et Al.*, Preparation and Characterization of Paraffin/Mesoporous Silica Shape-Stabilized Phase Change Materials for Building Thermal Insulation, *Materials*, 14 (2021), 7, 1775
- [2] Cao, M., Architecture and Application of Intelligent Heating Network System Based on Cloud Computing Platform, *Thermal Science*, 25 (2021), 4B, pp. 2889-2896
- [3] Kiuchi, N., et al., Model Study of Floodproofing Plans and Their Cost-Effectiveness Evaluation of Premises Occupying 1st Floor of an RC Building, *AIJ Journal of Technology and Design*, 29 (2023), 71, pp. 453-458

- [4] Zhan, B., *et al.*, Investigation on the Uncertainty Analysis of Heat Meters with a Novel Method of Integral Calibration, *Journal of Thermal Analysis and Calorimetry*, 148 (2023), 14, pp. 6989-7001
- [5] Zhao, C., *et al.*, A Critical Review of the Preparation Strategies of Thermally Conductive and Electrically Insulating Polymeric Materials and Their Applications in Heat Dissipation of Electronic Devices, *Advanced Composites and Hybrid Materials*, 6 (2023), 1, pp. 1-26
- [6] Xia, R., *et al.*, Transparent Wood with Phase Change Heat Storage as Novel Green Energy Storage Composites for Building Energy Conservation, *Journal of Cleaner Production*, 296 (2021), Feb., 126598
- [7] Lamy-Mendes, A., *et al.*, Progress in Silica Aerogel-Containing Materials for Buildings' Thermal Insulation, *Construction and Building Materials*, 286 (2021), 2, 122815
- [8] Petrtlova, R., Matej, J., Waterfront Character Areas as the Key Elements in Building the City – River Relationship, *International Review for Spatial Planning and Sustainable Development*, 10 (2022), 2, pp. 19-37
- [9] Fu, H., Thermal Energy Constant Temperature Control System of Building Energy System Based on Dynamic Analysis Method, *Thermal Science*, 25 (2021), 4B, pp. 2881-2888
- [10] Feng, X., Reliability Optimization Design of Intelligent Mechanical Structure for Waste Heat Recovery, *Thermal Science*, 27 (2023), 2A, pp. 1083-1090